Journal of Molecular Liquids, 25 (1983) 211—260
Elsevier Science Publishers B.V., Amsterdam — Printed in The Netherlands

A REVIEW AND COMPUTER SIMULATION OF THE STRUCTURE AND DYNAMICS OF LIQUID CHLOROFORM

M. W.EVANS

Chemistry Department, University College of Wales, Aberystwyth, Wales SY23 1NE (Gt. Britain)

(Received 17 September 1982)

ABSTRACT *

Over a hundred recent papers on the structure and dynamics of liquid chloroform have been analysed using computer simulation to produce reference numerical data from a model of the pair potential. A considerable amount of the available experimental data is contradictory or restricted in scope. Particularly, there is confusion about the role of collision-induced scattering, the nature of the internal field correction, rotation-vibration coupling, vibrational cross-correlation, and the anisotropy of $CHCl_3$ molecular diffusion.

The computer simulation suggests, for example, that the anisotropy of the rotational diffusion is opposite in sense to indications from NMR relaxation, based on the simple model of Langevin/Euler. Atom-atom p.d.f.'s from the simulation are compared with those of Bertagnolli [1] from neutron and X-ray diffraction. This is the first comparison of its kind and produces satisfactory, but not detailed, agreement. Data concerning orientational correlation times are summarised in tabular form from infra-red, far infra-red and dielectric absorption, Raman and Rayleigh scattering, NMR relaxation, Brillioun scattering and electric field

*EMLG Study Document by the Scientific Coordinator.

0167-7322/83/$03.00

induced anisotropy. These data are compared with results from the computer simulation.

The data survey and simulation both point to the need for a coordinated effort at obtaining more accurate and wider ranging data, and to develop and improve the currently available theoretical and data-reduction methods.

INTRODUCTION

The structure and dynamics of liquid chloroform have been studied intensively over the last decade with a variety of spectroscopic methods. In this review article we aim to coordinate the data available in over a hundred recent papers using the technique of site-site computer simulation as a theoretical basis upon which to construct a variety of data from a model of the pair potential. The structure of the liquid may then be investigated with atom-atom pair distribution functions, obtainable from neutron and X-ray scattering, and the dynamics with a variety of autocorrelation functions obtainable in principle from the frequency dependence of various spectral features.

Structure of Liquid Chloroform at 293K, 1 bar

The structure has been investigated by X-ray and neutron scattering on the isotropic species $CHCl_3$, $CDCl_3$, $CD^{35}Cl_3$ and $CD^{37}Cl_3$ by Bertagnolli et al [1-5]. Four independent neutron scattering experiments have been carried out on the species $CDCl_3$, $CD^{35}Cl_3$, $CD^{37}Cl_3$ and $CHCl_3$ (natural abundance). Based on these data, it is possible [1] to obtain some of the six atom-atom pair distribution functions of chloroform. An atom-atom p.d.f. is the probability of finding an atom of species A on molecule 1 given the position of atom B of molecule 2. It is also possible to build up these functions from a computer simulation using a site-site potential, where the total molecule to molecule pair potential is constructed from the twenty-five atom-atom interactions between each pair of chloroform molecules. In the absence of an experimentally-derived pair

potential for chloroform a convenient, but semi-empirical, representation of atom to atom interaction is the Lennard-Jones function. The site-site idea is maintained if the electrostatic part of the pair-potential is represented by point charges localised on each atom. This leaves aside any consideration of polarisability or electrostatic induction of all kinds. In the Rayleigh-Schrodinger expansion of basic quantum theory these effects are not pair-additive, atom-wise or molecule to molecule. In the results section we compare the date from our computer simulation with the atom-atom p.d.f.'s isolated, after much effort, by Bertagnolli and co-workers. These are specifically the carbon-carbon p.d.f. (the g_{oo}^{ooo} function [1]), the chlorine-chlorine p.d.f. and the sum of the Cl - H and Cl - C p.d.f.'s given in ref [1]. The other p.d.f.'s are also obtainable separately by computer simulation. As far as we know this is the first comparison of its kind for a dipolar polyatomic.

Hoheisel et al [7] have simulated the g_{oo}^{ooo} (spherically symetric) function for chloroform with an isotropic 18 - 6 Lennard-Jones function, and have obtained satisfactory agreement, but not detailed agreement, at 293K. This atom-atom p.d.f. corresponds to our carbon to carbon p.d.f. compounded with the anisotropic part of the interaction potential. The radial distribution function was calculated by Hoheisel et al [7] with the RISM theory of Weeks et al (see ref. [8]) and good agreement found with the molecular simulation [9]. Chloroform is therefore unusually well studied as regards its structural details, and in this review we aim to see to what extent our understanding has been improved by the intense experimental effort on diffraction from various isotopic species of this molecular liquid.

Molecular Dynamics in Liquid Chloroform

These have been investigated by a variety of techniques, each of which uses particular assumptions and approximations in the data-reduction (the process of transforming raw spectral data into correlation functions,

correlation times etc.). These methods have been developed and applied to chloroform by an increasing number of investigations in the last ten years, and we restrict our review to this period. There are many hundreds of papers prior to this time which are rather less relevant to the subject of this review. Among these are some important key papers to which we shall refer.

Infra-red Absorption, Raman and Rayleigh Scattering

The early papers in these fields have been summarised conveniently by Brodbeck et al [10] in terms of correlation times. We compare these with our computer simulation results in table (1) (see also refs [11] to [18]). Brodbeck et al reveal the spread in the first and second rank orientational correlation times from various sources and comments further on the need for a proper definition of "correlation time". The first rank orientational correlation times listed by Brodbeck et al vary from 2.3 ps to 4.0 ps according to definition. In this review, we define the correlation time as the area beneath the relevant correlation function. In the context of our computer simulation this is always an autocorrelation function [19]. According to Brodbeck et al a comparison of relaxation times from the ν_1, ν_2 and ν_3 (A_1 symmetry) fundamentals of chloroform reveals rotation/vibration coupling to be insignificant. This is discussed further in ref. [19], chapter 6. They proceed to apply Bratos' theory [20,21] and test it with isotropic dilution. Corrections are applied for isotropic broadening, band combination effects, hot bands and what the authors term hydrogen-bonding, which is "very weak" (sic).

The broadening of the ν_1 (C - H stretch) fundamental in liquid chloroform leads to an orientational autocorrelation function for the tumbling of this axis (the C_{3v}, or dipole, axis). Brodbeck et al list first rank (infra-red) and second-rank (Raman) correlation times for this motion. For natural abundance $CHCl_3$ the former vary from 2.3 to 2.9 ps, apparently according to depolarisation ratio [10] and the latter from various sources from 1.3ps [17]

Table 1

Some Correlation Times and Related Data for Liquid Chloroform

Technique	Correlation Times (At ambient T unless otherwise indicated)	Computer Simulated Corr. Times (293K).
Dielectric Relaxation	Pure liquid [22-24]: 5.4ps to 6.4ps Dilute n-hexane solution: 2.9ps [22-24] Dilute CCl_4 solution: 6.1ps [22-24] Pure liquid [121]: 4.7ps to 6.2ps Dilute cyclohexane soln: 3.2ps [122] 10% v/v decalin soln: 4.3 ± 0.3ps [43] Dilute CCl_4 soln: 5.0ps [122] Pure liquid [31] 6.0ps (294K) 17.0ps (223K)	Pure chloroform at 293K, 1bar. First rank autocorrelation time of the dipole (C_{3v} axis) unit vector $\underline{e}_3$ [120]. $\tau_1(\underline{e}_3) = 3.6$ps
Nuclear Magnetic Resonance Relaxation	^{35}Cl transverse nuclear quadrupole relaxation times [87]: 2.0ps (pure liquid); 1.8ps (1.3 n-hexane); 3.4ps (1.3 CH_2I_2)	A weighted mean [19] of three second rank correlation times of unit vectors $\underline{e}_1$, $\underline{e}_2$ and $\underline{e}_3$ in the principal moment of inertia axes. $\tau_2(\underline{e}_1) = \tau_2(\underline{e}_2) = 1.5$ps $\tau_2(\underline{e}_3) = 1.3$ps
	^{13}C spin-lattice relaxation time [88]: 1.60ps	$\tau_2(\underline{e}_3) = 1.3$ps
	D nuclear quadrupole relaxation [89]: 1.84ps	$\tau_2(\underline{e}_3) = 1.3$ps
	Spin-spin relaxation: 1.5ps [34]; 1.74ps [13]	$\tau_2(\underline{e}_3) = 1.3$ps
	Proton spin-lattice relaxation [92]: 1.39ps (298K); 3.0ps (219K); 1.07ps (363K)	A mean of [19]: $\tau_2(\underline{e}_3) = 1.3$ps $\tau_2(\underline{e}_1) = \tau_2(\underline{e}_2) = 1.5$ps

Table 1 (continued)

	Intermolecular (translational) correlation times [92]: τ_c: 80.5ps (298K); 263ps (219K); 52.2ps (363K)	Calculated in the extreme narrowing limit from the centre of mass velocity [120] correlation time (τ_v) using $\tau_c = ma^2/(12kT\tau_v) = 2.1$ps m = mass of mol., a = eff. radius.
	A combination of D and ^{35}Cl nuclear quadrupole relaxation [89]:	
	$\tau_{\perp}$(spinning) = 0.92ps $\tau_{\perp}$ (tumbling)] 1.8ps	$\tau_2(\underline{e}_1) = \tau_2(\underline{e}_2) = 1.5$ps $\tau_2(\underline{e}_3) = 1.3$ps
	^{13}C, nuclear Overhauser enhancement [94], $^{13}C-^{1}H$: 1.26 ± 0.04ps	$\tau_2(\underline{e}_3) = 1.3$ps
Infra-red Bandshape Analysis	N.B. These orientational times have been derived assuming that rotation/vibration coupling is negligible; but see [42].	
	$\nu_1(A_1)$ (C-H stretch) : 2.3ps [10] to 2.9ps [10]	$\tau_1(\underline{e}_3) = 3.6$ps
	$\nu_1(A_1)$: variation with defn. of correlation time [10]: 2.3ps to 4.0ps Area defn. = 2.6ps [10]	$\tau_1(\underline{e}_3) = 3.6$ps (area defn.)
Raman Bandshape Analysis	$\nu_1(A_1)$ (C-H stretch) : 1.5ps [10]; 1.5ps [11[; 1.97ps [13]; 1.2ps [15]; 1.3ps [17]; 1.7ps [10]; 1.59ps [142]; $\nu_1(A_1)$ ($CDCl_3$): 1.7ps [15]; 1.96ps [16]; 1.8ps [18]; 5.1ps [10]; 2.0ps [15]; 3.1ps [17]	$\tau_2(\underline{e}_3) = 1.3$ps
	$\nu_2(A_1)$ (C-Cl stretch) : 2.4ps [15]; 1.8ps [17]; 1.4ps [11]; $\nu_2(A_1)$ (C - Cl stretch : $CDCl_3$): 2.4ps [15]; 1.85ps [16]; 3.4ps [15]; 4.4ps [17].	$\tau_2(\underline{e}_1) = \tau_2(\underline{e}_2) = 1.5$ps $\tau_2(\underline{e}_3) = 1.3$ps

	$\nu_3(A_1)$ (symm. CCl bend, $CDCl_3$): 5.3ps [11]; 6.8ps [15]; 6.6ps [17]	
	Variation of $\tau_2(\underline{e}_3)$ with def. [10]: 1.3ps to 1.5ps. Area defn. = 1.3ps	$\tau_2(\underline{e}_3)$ = 1.3ps (area defn.)
	$\nu_1(A_1)$ [45,48]: 1.45 ± 0.15ps (pure $CHCl_3$)	$\tau_2(\underline{e}_3)$ = 1.3ps
	$\nu_1(A_1)$ [41,48]: 1.20 ± 0.15ps (20% mole fraction in CCl_4) 2.61 ± 0.15ps (33% m.f. in $(CD_3)_2CO$)	
Depolarised Rayleigh Scattering	τ_r = 1.7ps [12]; $\tau_r(CDCl_3)$ = 2.9ps [18]	A weighted mean [19] of $\tau_2(\underline{e}_1) = \tau_2(\underline{e}_2)$ = 1.5ps $\tau_2(\underline{e}_3)$ = 1.3ps (N.B. these are <u>auto</u> correlation times)
	τ_r] ±0.2ps (3.2)[33](1bar)	
	τ_r = 5.5(5) ± 0.2ps (at 205MPa [33]).	
	τ_r = 2.95ps [34] τ_r = 1.74ps (in 20% CCl_4 [34])	
	τ_g = 0.24ps [35] (far wing Gaussian).	
Far Infra-red Absorption	<u>Experimental Peak Frequencies/cm^{-1}</u>	<u>S</u>imulated peak frequency, ν_{max}(sim.) = 31cm^{-1}. (N.B. from the rotational velocity <u>auto</u> correlation function).
	$\bar{\nu}_{max}$ = 36cm^{-1} [85]	
	= 45cm^{-1}[40]	
	= 38cm^{-1}[26]	
	$\bar{\nu}_{max}$ = 30cm^{-1}[65] (in 10% decalin v/v)	
	$\bar{\nu}_{max}$ = 39cm^{-1}[65] (in 10% decalin v/v)	
	$\bar{\nu}_{max}$ = 25cm^{-1}[65] (in 10% n pentane v/v)	
	$\bar{\nu}_{max}$ = 37cm^{-1}[65] (in 10% diphenylmethane v/v)	Simulated peak frequency in pure $CHCl_3$ at 293K, 1bar = 31cm^{-1} (fig. 4).
	$\bar{\nu}_{max}$ = 50cm^{-1}[43] (in 10% v/v decalin, supercooled to 110K)	

Table 1 (continued)

	Peak of Rayleigh second moment [32] = $45cm^{-1}$
	Peak of $\nu_1(A_1)$
	Raman second moment [29] = $50cm^{-1}$
Electric-Field Induced Birefringence	Kirkwood factor g_1 = 1.4[95] Higher-order correlation factors: g_2 = 1.7, g_3 =-0.4 The factor g_1 compares with g_1 = 1.32[40] from f.i.-r. analysis and g_1 = 1.25[26] from dielectric permittivity

to 1.7 ps [10]. The second rank (Raman) times vary from 1.3ps to 1.5ps according to definition [10]. The Raman orientational correlation times from the ν_2 (sym. C - Cl stretch) range from 1.4ps [11] to 2.4ps [15]. These are affected by spinning and tumbling of the C_{3v} axis.

It is usually accepted in these early papers that orientational correlation times from infra-red and Raman bands are auto-correlation times, whereas the equivalent times from dielectric relaxation (first rank) and depolarised Rayleigh scattering (second-rank) reflect the motions of many molecules, involving cross-correlations [19]. It is often the practice to compare Raman and Rayleigh orientational correlation times, or alternatively, infra-red and dielectric correlation times in an attempt at discerning a statistical correlation between the movements of different molecules. Soussen-Jacob et al [14] have shown that the dielectric relaxation times [22-24] available to them varied from 5.4ps to 6.4ps in pure $CHCl_3$, and from 2.9ps to 6.1ps on dilution in n-hexane and CCl_4 respectively. Systematic measurements

have been reported in the dielectric/far infra-red region by Gerschel et al [25-27]. Gerschel and Brot [27] measured the static permittivity of chloroform along the gas-liquid coexistence curve to the critical point. The static (classical equilibrium [19]) Kirkwood factor g depends on the steric configuration, especially on the orientation of the dipole axis in relation to the shape of the molecule. The value of g for the liquid phase of chloroform changes with temperature, and approaches unity at the critical point. Its value is unity at all densities in the coexisting vapour, and about 1.25 in the liquid over a range of temperature, as estimated from the Kirkwood-Frohlich equation (ref. [19], chapter 3). The Onsager formula predicts with accuracy the the dielectric static permittivity as a function of temperature throughout the critical region. The evolution of the dielectric relaxation time has been reported by Gerschel [22] up to the critical temperature. It appears to follow an Arrhenius law over a wide range of temperatures, but then reveals a definite temperature at which the liquid-like rotational process evolves into a gas-like process, where the rotational motion is relatively freer. There is no particular critical phenomenon, such as observable opalescence in the far infra-red.

Therefore it seems that the technique of dielectric relaxation alone, applied over a range of state points, can provide much more information on the dynamical cross-correlation in liquid chloroform than can a simple comparison of, for example, Raman and Rayleigh correlation times at one state point. The majority of papers on Raman spectroscopy in liquid chloroform do not use density as a variable. However, Jonas et al [28-30] have made a systematic study of liquid chloroform under hydrostatic pressure. Schroeder and Jonas [29] use second moment analysis [19] to reveal that "collision induced effects", play a role in making the measured rotational second moment of the $\nu_1(A_1)$ band in liquid $CHCl_3$ and $CDCl_3$ density dependent [see ref. 19, chapter 11, for details of the parallel far infra-red phenomenon]. The collisional contribution to the second moment decreases with increasing density (up to a pressure of 4.5 kbar,

but is only adequately revealed by constructing the second moment spectrum from the far wing of the Raman line. The results of Schroeder and Jonas contradict those of van Konynenberg et al [12], who have suggested that there are no collisional contributions to the rotational second moment. Schroeder and Jonas also studied the depolarised Rayleigh wing up to 4kbar and out to about 200 cm^{-1}. The results are analagous with the Raman spectra, in that several clearly defined regions exist. From zero frequency to about 30cm^{-1}, the spectra seem to be lorentzian, while beyond, the decay seems to be exponential with frequency. The Raman bandshapes drop off fairly rapidly at 80 cm^{-1} (faster than ω^{-3}) while the Rayleigh band shapes continue to about 180 cm^{-1} before dropping off rapidly. This is interpreted in terms of many-body collision effects at short times (the range 0.03 to 0.5ps). Schroeder and Jonas emphasize the usefulness of second-moment analysis. In the far infra-red [19] such analysis is effectively standard practice, and in our simulation we will produce the far infra-red second-moment at 293K. We have mentioned that our model cannot take into account collision induction, so that the effect of the latter on the far infra-red spectrum can be checked by comparing the band-shape (power absorption coefficient) produced by the simulation with the experimental data [31] in the far infra-red. Lund et al [32] have shown that the Rayleigh and far infra-red second-moment spectra peak at the same frequency (45 cm^{-1}) and are similar in shape. Lund et al attribute the origin of both types of spectra to molecular torsional oscillation, and do not mention collision-induced effects. It would be interesting to study the far infra-red second-moment spectra as a function of hydrostatic pressure. Some data in this field have been supplied by Gerschel et al [22, 25-27] along the gas-liquid coexistence line, and are reviewed in the far infra-red section. Claesson et al [33] have reported Rayleigh correlation times (obtained from spectral half-widths) to 205 MPa. These vary linearly from 3.2 $\pm$ 0.2 ps at 0.1MPa (1 bar) to 5.5(5) $\pm$ 0.2 ps at 205MPa. The dependence of the rotational relaxation time on bulk viscosity at constant temperature is also linear, with a non-zero

intercept. Cleasson et al compare their results with high pressure NMR and Raman data and discuss the effect of pressure on pair correlations. They compare their results with the Raman and NMR data of Campbell et al [13] on rotational relaxation times. The latter cut the zero viscosity axis differently, and do not lie on the same straight line as the Rayleigh correlation times. The NMR and Rayleigh correlation times of Alms et al [34] are also included on this plot by Claesson et al. Pair correlations on the basis of these measurements seem to be significant in chloroform. At higher pressures, the Rayleigh light scattering and Raman rotational relaxation times approach each other. This suggests either the magnitude of the static and dynamic contributions to the pair correlations are changing with pressure or the approximation used to obtain the single particle Raman rotational relaxation times from polarized and depolarized Raman spectra are not valid at high pressure, or both. Alms et al showed that the depolarised Rayleigh times were strongly concentration dependent for chloroform, suggesting that pair correlations are affecting the data at high concentrations. As we have mentioned, a different interpretation (in terms of collision-induction) has been put on the same set of results by Jonas and coworkers [29]. Alms et al report a dynamic correlation factor of 1.0 for pure liquid chloroform at 1 bar which can be compared with the (static) Kirkwood correlation factor of 1.25 obtained by Gerschel et al [25-27] in the liquid over a range of densities along the gas-liquid coexistence line. Claesson et al [33] point out that the Raman and NMR correlation times do not agree, except at atmospheric pressure. A comparison of the Rayleigh times (τ_ω) with the Raman times (τ_2) shows that pair-correlations are decreasing as hydrostatic pressure is increased which conflicts with the view of Schröder et al [29]. In the absence of collision-induced effects, τ_ω should increase faster than τ_2, according to Claesson et al, simply due to the increase in the number of scatterers (N) in the scattering volume. However, this is not observed [33] and a possible explanation could be given in terms of the collision-induction hypothesis of Schroeder et al [29]. Collision-

induction is dependent on a power of N, as in the far infra-red [19, chapter 11]. Claesson et al mention the possibility of "non-orientational relaxation processes" (sic) at high pressures. A computer simulation will help clarify these points.

Kamogawa [35] has reported a study of $CHCl_3$ in CCl_4 by depolarised Rayleigh scattering. The relaxation times of the solutions were found to be independent of concentration, the integrated intensities showing a linear dependence on concentration. This seems to contradict the results of Alms et al [34] for the central part of the overall spectrum. Kamogawa analyses his spectrum in terms of several different relaxation times, calculated from the half-widths of the central and far-wing portions. This over-complicates the problem, in our opinion, and the technique of computer simulation produces the complete frequency range from a given model of the pair potential. Analogously, the entity for analysis in low frequency absorption spectroscopy is the complete zero to terahertz sweep [19]. Kamogawa comes to the opposite conclusion to Schröder et al [29] concerning collision induced effects in the far Rayleigh wing. These are found to be negligible on the basis of the "observed relaxation time" (sic), its concentration dependence and that of the integrated intensity (A) of the spectrum, which is linear in N, the number density of the chloroform molecules. Kamogawa asserts that if the spectrum is caused by a binary collision process, A should be proportional to N^2. However, the fact that A is not proportional to N^2 [35] is no evidence for the absence of collision induced effects. Analysis of far infra-red collision-induction processes shows [19, chapter 11] that the latter are not pairwise additive in molecular terms, and not proportional to N^2 in the liquid phase. This is very clearly shown in the case of nitrous oxide [19, chapter 11]. The far infra-red evidence does agree in some respects with Kamogawa's analysis in that the integrated absorption intensity (the area beneath the power absorption coefficient) of solutions of chloroform is linear in N. If collision-induction is important then its N dependence has to be the same on the evidence of dilution as that of the non-

collisional, reorientational process (which we simulate by computer in this work). There is also available some clear evidence from the far infra-red [19, chapter 11] that the band-shape and frequency of maximum absorption of the collision-induced process, when isolated from the permanent dipole absorption band as in N_2O, is displaced from the latter and obviously distorts it. If we now take into consideration the work of Lund et al [32], who construct the second moment of the Rayleigh wing spectrum and compare it with the far infra-red spectrum, no clear evidence of distortion is apparent, the bandshapes from both spectral sources being similar and peaking at the same frequency ($45cm^{-1}$) in pure liquid chloroform at ambient temperature and pressure. If the computer simulation also comes up with the same or similar band-shape, we must conclude that collision-induced effects are either small or have the same frequency dependence as the underlying reorientational process at ambient temperature and pressure. Schröder et al [29] (their figure 3) construct the second moment of the far wing of the Raman ν_1 mode at pressures up to 4kbar. This peaks at 30bar at about $50cm^{-1}$ (cf. the $45cm^{-1}$ of Lund et al [32] and is noticeably similar in appearance to the zero-THz spectrum (e.g. [22, 25-27, 36] at 1bar, ambient temperature. The area of this curve decreases rapidly with increasing number density (N) as the hydrostatic pressure is increased to 4 kbar at 303K. On this basis Schro et al conclude that multi-body collision induction is responsible for the shape of the second moment Raman spectrum of the chloroform ν_1 mode. A relevant analysis of the far infra-red, purely collision-induced, spectrum of liquid Cs_2 to 12kbar has been reported by Evans et al [19, chapter 11]. The frequency shift and number density dependence of the integrated absorption are both opposite to that observed by Schröder et al [29] for chloroform (Raman ν_1) as a function of hydrostatic pressure. In this work we shall simulate the far infra-red spectrum of pure liquid chloroform at 4.5kbar, 303K to estimate the dependence upon hydrostatic

pressure of the non-collisional dynamical process. This is reported in a later paper. The Rayleigh wings reported by Schröder et al [29] behave similarly to the Raman ν_1 wing, but the second moment spectra are not illustrated. It is clear, however, that the integrated intensity per molecule of the Rayleigh spectrum decreases in the wing portion as the pressure is increased to 4kbar from 30bar at 303K. However, in neither the Raman nor the Rayleigh case is it clear how the low frequency part of the scattered intensity (close to the exciting line) behaves as a function of pressure. The complete (zero to herahertz) range should be the entity for analysis, and the overall integrated intensity is dominated by the low frequency part (being several orders of magnitude more intense than the far wing). Second moment analysis (as in the far infra-red) totally suppresses the low frequency contribution. Analysis should take into account both the zeroth and second moments, together with higher moments [19] if available. Only then will a satisfactory picture of the various contributory processes begin to emerge.

To end this part of our discussion on collision-induction in liquid chloroform we point out that the results of Schröder et al [29] can be interpreted differently: in terms of dimer formation. If the population of dimers (weakly hydrogen-bonded [37]) were to increase with hydrostatic pressure, the effective moment of inertia of C-H scattering units would increase. This would show up as a decrease in the second moment of the Raman ν_1 band. Suzuki et al [37] have reported that the infra-red ν_1 band is pronouncedly asymmetric, with a remarkable tailing on the high frequency side at ambient temperature and pressure. They point out that the integrated intensity of the chloroform infra-red ν_1 band increases from 11 to 198 cm^2 m_{ol}^{-1} on passing from the gas to the liquid phase. This is interpreted usually in terms of hydrogen-bonding [38]. Rothschild et al [39] reject this hypothesis on the basis of their infra-red and Raman data and several

subsequent studies [40,10,28,30,41], including those of Schröder et al. have been been based, according to Suzuki et al. [37], on the assumption that the ν_1 band is homogeneous (i.e. unaffected by H-bonding). Suzuki et al. point out that the infra-red ν_1 fundamental is strongly asymmetric in both $CHCl_3$ and $CDCl_3$ and that its width in is significantly the narrower. Moradi-Araghi et al [41] have considered that vibration-rotation coupling [42] is stronger for the ν_1 mode in $CHCl_3$ because of anharmonic terms in the vibrational hamiltonian, but Suzuki et al [37] reinterpret this as the formation of dimers through hydrogen-bonding. They break down the infra-red ν_1 profile into three bands, at 3017.5 (1), 3028 (2) and 3062 (3) cm^{-1} for $CHCl_3$ and 2252, 2259 and 2284 cm^{-1} for $CDCl_3$. Band (1) is assigned to the dimer species, band (2) to the monomer and band (3) to an independent source, such as a combination mode or "pseudo-lattice" vibration. The intensity of band (1) is reported to decrease relative to band (2) upon dilution in CCl_4, their positions remaining constant. The peak frequency and absolute intensity of band (2) are closer to the values for gaseous chloroform, (where it is assumed that only monomers exist). It is precisely this high frequency ν_1 profile that is reported by Schroeder et al [29] in their Raman studies. From their analysis, Suzuki et al calculate [37] that 44% of the molecules in pure liquid $CHCl_3$ at ambient temperature and pressure are bound into dimers. They also comment on the uncritical use of the intensity of vibrational modes for the study of intermolecular interactions. They assert that a vibrational spectrum in the condensed plane is composed, in principle, of <u>different</u> band maxima and intensities corresponding to different species of monomer and dimer. However, it should be pointed out that there is little corroborative evidence of either association or H-bonding in liquid chloroform from the dielectric and far infra-red rotational spectra conveniently summarised by Gerschel [36]. For example, the static Kirkwood factor, g, remains near unity along the gas-liquid coexistence curve [26,27], and there is little sign of association

in the far infra-red [19, chapter 4], in sharp contrast to liquids such as acetonitrile, aniline or the alcohols [43]. It seems clear, however, that the infra-red, and possibly the Raman ν_1 fundamentals in $CHCl_3$ and $CDCl_3$ liquids are asymmetric. It is by no means clear therefore that the results of Schröder et al [29] can be ascribed unequivocally to collision-induction. The Raman ν_1 stretch has been investigated recently by Tanabe et al [44] in different solvents. The bandwidth of solutions of $CHCl_3$ in water are about twice as large as those in the neat liquid, in CCl_4, or C_6D_{12}. This contrasts with the behaviour of solutes such as CH_3OH, CH_3CN, CH_3NO_2 and acetone. This provides unambiguous evidence that the H-bonding between $CHCl_3$ and H_2O solvent molecules is considerably weaker than in the other cases. On this evidence, the H-bonding between like $CHCl_3$ molecules in the pure liquid must be very weak, amounting to no more than a slightly increased probability for certain configurations over others. There is no significant evidence for dimer formation in the X-ray and neutron diffraction atom-atom p.d.f.'s of Bertagnolli et al [1-6]. A more likely explanation for the asymmetry of the ν_1 mode is therefore inhomogenous broadening, recently discussed by Laubereau et al [45-47] who find that rotational coupling with vibration, Fermi resonance and resonance energy transfer strongly affect the vibrational population lifetime on a picosecond time-scale. Inhomogeneous broadening should therefore affect the spontaneous Raman data of Schröder et al [29], whose second-moment behaviour could be explained in terms of a decrease of inhomogeneous broadening with increasing hydrostatic pressure. This assumes that stimulated (Laubereau et al.) and spontaneous (Schröder et al.) Raman processes behave similarly in this respect. In one sense, the inhomogeneous broadening and H-bonding schools of thought can be reconciled as being both descriptions of the anisotropy of local environment. We can investigate this by computer simulation using atom-atom p.d.f.'s [1].

Moradi-Araghi et al [48] have recently reported in detail a variety of reorientational correlation times from the polarised and depolarised Raman spectra of the ν_1 band in neat $CHCl_3$, $CDCl_3$ and solutions in CCl_4, acetonitrile and acetone. The second-rank orientational correlation functions decay more rapidly in CCl_4, but more slowly in the two dipolar solvents. This is contrary to expectations based on classical rotational diffusion theory [19, chapters 1 and 2]. An interpretation is given in terms of specific solute-solvent interactions for loss of reorientational correlation and vibrational dephasing in each solvent. Moradi-Araghi et al [41, 48] factorise rotation from vibration assuming that the two processes are statistically independent. This view is shared by Brodbeck et al [10] but not by van Woerkom et al [42]. As we have mentioned, Suzuki et al [37] interpret the anomalously large isotope effect on the ν_1 band when $CHCl_3$ is deuterated in terms of hydrogen-bonding and reject the interpretation of Moradi-Araghi et al. We have pointed out that there is little independent evidence for hydrogen-bonding in liquid chloroform but accept that the ν_1 band is asymmetric (i.e. inhomogenously broadened) in the far infra-red and stimulated Raman. If, for the sake of argument, we accept the factorisation of vibration from rotation employed by Moradi-Araghi et al, the second-rank reorientational correlation times vary from 1.45 ± 1.15 ps in pure $CHCl_3$ at room temperature and pressure to 1.20 ± 0.15 ps in 20% mole fraction $CHCl_3$ in CCl_4. These correlation times are not proportional to the bulk viscosity. A maximum correlation time of 2.61 ± 0.15 ps is recorded for a 23% m.f. solution of $CHCl_3$ in deuterated acetone. Vibrational dephasing is discussed in terms of the Kubo theory developed by Rothschild [49].

These interpretations must, however, be viewed with caution in the light of the careful and detailed paper by van Woerkom et al [42] who used isotope dilution methods to show that vibration is not statistically independent of

rotation in the infra-red spectra of liquid $CHCl_3$, $CDCl_3$ or $CHCl_3/CDCl_3$ mixtures. This point of view is shared by Laubereau et al for stimulated Raman scattering [45-47]. The conclusion reached by Brodbeck et al [10], that rotation/vibration coupling is negligible in $CHCl_3$ and $CDCL_3$, conflicts diametrically with that of van Woerkom et al [42]. Future computer simulations will aim to resolve this problem using a classical expression for the harmonic or anharmonic vibration of the C - H bond dependent on the angular momentum of the diffusing $CHCl_3$ molecule.

The interpretation of isotropic Raman band contours in terms of vibrational auto-correlation functions has recently been questioned in other contexts by Wertheimer [50]. He looks theoretically at several processes which may affect the broadening of a Raman band in the liquid state. The purely intramolecular process includes vibration-rotation coupling, and vibrational depopulation from excited quantum states. On top of these, and neglected in the majority of papers mentioned above, the broadened liquid state Raman band contains information on relaxation processes which are intermolecular in origin, involving two or more molecules. These processes include resonance transfer (vibrational exciton hopping) and pure dephasing (transition frequency fluctuations). The rotovibrational correlation function obtained from a Raman band is a collective correlation function according to Wertheimer, and not a pure autocorrelation function. Homogeneous band-widths are interpretable therefore in terms of a sum of these processes, together with cross terms from the interference mixing of pure dephasing and resonance transfer processes, and of resonance transfer transitions involving different pairs of molecules. Resonance transfer contributions are removed by dilution, conveniently isotopic dilution, so that an estimate of the relative importance of each contribution can be made [50]. In this context, a study of $CHCl_3/CDCl_3$ mixtures under hydrostatic pressure [29] should prove revealing as to what extent resonance transfer is responsible for the second moment behaviour monitored

by Schröder et al [29] separately in $CHCl_3$ and $CDCl_3$. This would also allow the separation, according to Wertheimer, of the individual broadening factors of an isolated band. As we have seen, there is evidence to suggest that the ν_1 mode of $CHCl_3$, and that of $CDCl_3$, is asymmetric, and in one sense made up of weakly-separated bands (Suzuki et al [37]). In the case of weakly separated bands whose origins can be traced to the equivalent excitations in isotopic mixtures, Wertheimer provides a series of theoretical results. The widths of the vibrational self-correlation functions are found to be essentially independent of concentration, because the nearly resonant transfer involving molecules of different types is almost as fast as the resonance transfer between molecules of the same species. The collective modes, involving two or more molecules, are dynamically coupled. Wertheimer derives these results using Zwanzig-Mori theory [19, chapters 1-5, 9, 10] on a 2 x 2 vibrational correlation matrix in terms of which the Raman spectrum of the coupled modes can be described. Vibration-rotation (intramolecular) coupling is neglected. In the first approximation this can be treated, as pointed out by Wertheimer, by making use of vibrational energies which depend parametrically on the molecular angular momentum [51], contrary to the Born-Openheimer approximation. The Zwanzig-Mori theory used by Wertheimer has recently been greatly developed in other contexts by Grigolini et al (for a discussion of basic details see ref. [19], chapters 9 and 10).

Wertheimer employs pair-potentials of the form $\phi^{JK}(\underline{x}_j, \underline{\Omega}_j, \underline{q}_j; \underline{x}_k, \underline{\Omega}_k, q_k)$ to describe the molecular interaction. Here $\underline{x}_j$, $\underline{\Omega}_j$ and $\underline{q}_j$ describe the position, orientation and vibrational deformation, respectively, of a molecule j of species J. It is clear, therefore, that his approach is similar to the molecular dynamics simulation used in this work, except that we do not take vibrational motion into account. It is equally clear, then, that what Wertheimer terms "collision-induced" processes is not what is meant by "collision-induction" in the far infra-red ([19], chapter 11). The latter

is a multi-body process resulting in the appearance of temporary molecular dipoles in a species such as benzene which is normally non-dipolar. Similarly, collision-induced Rayleigh scattering ([19], chapter 11), is a multi-body non pair-additive, process resulting in the appearance of temporary polarisability anisotropy in an otherwise isotropically polarizable species such as CCl_4. There are similar non-pair-additive processes which give rise to temporary transition-dipoles (infra-red collision induction) or temporary polarisability components (spontaneous - Raman collision induction). These processes all involve the molecular polarisability anisotropy, explicitly ([19], chapter 11). Wertheimer assumes that the dynamic isotropic polarizability α of the liquid system is a superposition of the polarizabilities of its individual molecules [52, 11, 40] in a pairwise-additive manner (his eqn. (15)). This contradicts the Rayleigh-Schrodinger picture of basic quantum-mechanics, where polarisability is clearly not molecularly pairwise additive [53].

Therefore, the "collision-induced" processes of Wertheimer, namely, pure-dephasing, resonant and non-resonant energy transfer and intramolecular depopulation, arise from what is known in other fields as cross-correlation - the statistical influence of the motion of one molecule on another. In the dielectric/far infra-red field this involves the reorientation of molecular dipoles, in the Raman and infra-red the cross-correlation of two vibrating, rotating and translating molecules leads to new and different effects. These are not what, for example, Schroeder et al [29] mean by collision-induced effects.

Wertheimer conveniently summarises the basic (and incorrect) assumptions usually made about vibration-rotation coupling and cross-correlations in the majority of papers in this field (his eqns. (42) to (44)). It is interesting to note from Wertheimer's eqn. (42) that he uses the number density (N) in the denominator. This disappears (his eqn. (44)) if ss-correlations are

neglected (on a pairwise additive basis). The results of Schro et al [29] could therefore be interpreted as showing the presence of cross-correlations in the ν_1 mode, because an increasing N (with hydrostatic pressure) could, in principle, cause the second moment to decrease according to the basic equation labelled by Wertheimer as his eqn. (42).

Experimental evidence for the presence of cross-correlations has been presented by Yarwood et al [54] for the ν_1 and ν_3 modes of acetonitrile, and numerical evidence by Oxtoby et al [55] from computer simulation in N_2. Wertheimer discusses cross-correlations in the ν_4 mode of $CHCl_3$ [50], and Grigolini gives a detailed review in ref. [19], chapters (9) and (10). Doege et al [56] have recently corroborated this evidence by studying the ν_1 mode of $CHCl_3$ in CH_3I solvent, where the bandshape is "drastically" broadened as the molecular environment changes.

The separation and characterisation of the multi-body collision-induced Rayleigh scattering in liquid chloroform has been discussed by Carlson et al [57], who come to the conclusion that approximately half of the scattering for a system of independent, non-interacting molecules, is dependent on $\gamma^2 = (3/2)\ \mathrm{Tr}\ (\hat{\underline{\alpha}}\hat{\underline{\alpha}})$ where $\hat{\underline{\alpha}}$ is the anisotropic part of the complete polarisability tensor of the molecule. It is therefore quadratic in $\hat{\underline{\alpha}}$, which is affected by cross-correlations (in the sense of Wertgeimer) and by transient, collision-induced perturbations (ref. [19], chapter 11). Carlson et al argue that the Kerr effect and Cotton-Mouton effect, on the other hand, are both dominated by terms which are linear in $\hat{\underline{\alpha}}$, and are relatively unaffected by collision-induced effects as a consequence. These authors develop an experimental method, based on interference filters, for estimating the collision-induced intensity of the depolarised Rayleigh spectrum. This is based in turn on the theory and analysis of Bucaro et al [58], who assume the collision-induction process to be caused by isolated binary collisions (specifically for CCl_4). Evans et al [19, chapter 11] show, however, that

this is not the case, by comparison of collision-induced far infra-red data (for nitrous oxide, for example, or for cyanogen or carbon dioxide) in the gaseous and liquid phase.

The method devised by Carlson et al [57] for separating the collision-induced intensity is the equation:

$$I_{HV}(\sigma) = I_{mol}(\sigma) + I_{col}(\sigma) \qquad (1)$$

where $I_{mol}(\sigma)$ and $I_{col}(\sigma)$ are the integrated intensities transmitted by the filter characterised by σ. $I_{col}(\sigma)$ is the collision induced part of the overall depolarised Rayleigh intensity $I_{HV}(\sigma)$. The integrals are evaluated with the theory of Bucaro et al [58], whose validity is doubtful [19]. Furthermore, the Kerr effect may be dominated by $\underline{\mu}^{T}\hat{\underline{\alpha}}\underline{\mu}$, where $\underline{\mu}$ is the permanent dipole moment [58], i.e. is quadratic in $\underline{\mu}$ and linear in $\hat{\underline{\alpha}}$, as Carlson et al point out, but the collision-induction process also affects $\underline{\mu}$, the permanent dipole moment, as we see in the far infra-red, where otherwise non-dipolar molecules absorb over a broad range of frequencies [19, chapter 11]. It is by no means clear therefore that the anisotropy data from the Kerr effect can be regarded as free of these induction effects. As Carlson et al point out, there is considerable confusion in the field of Rayleigh scattering about the expression that ought to be used for the internal field correction. Carlson et al themselves favour the square of the Lorenz-Lorentz factor (their eqn. (24)). The internal field correction has a considerable effect on the measured intensity, as in the far infra-red [43], where recent advances in understanding its role have been made by Bossis [59]. There is considerable uncertainty, therefore, about the role of collision-induction in the Rayleigh and Raman spectra of $CHCl_3$. Some authors [12,32,33,35] do not discuss it, or conclude it is to be negligible, others [29,57,58] find it to amount to as much as one half of the relevant spectral intensity. Computer simulation is an unambiguous means of determining the effect of collision induction on the bandshape, as in the far infra-red for example, but the intensity of the far infra-red,

Rayleigh, infra-red or Raman band under consideration is determined by extraneous factors such as the (dynamic) internal field [19, chapter 3], making it difficult to assign any intensity measurement unambiguously to the effect of collision-induction. If the bandshape generated by the computer matches, for example, the far infra-red bandshape well, then the collision-induction process is either negligible or must have the same frequency dependence as the reorientational process. The latter is not the case in the gas state [19, chapter 11], and from independent evidence on non-dipolar liquids is unlikely to be the case in dipolar liquids such as $CHCl_3$. This argument is probably transferable to Rayleigh scattering, especially in the light of the similarity between the far infra-red and Rayleigh second moments discovered by Lund et al [32]. The final conclusion is likely to be, as in the far infra-red, that the intensity of Rayleigh scattering per molecule squared decreases considerably on passing from the gas to the liquid state, indicating a concellation effect of symmetrically disposed neighbouring fields on a central reference collision induced property. In this respect more work is needed on intensity measurements by Rayleigh scattering on compressed vapours such as $CHCl_3$, or along the gas-liquid coexistence line as indicated for the far infra-red by Gerschel [36]. Ho et al [60] have indicated the need for a theory of "close encounters" in the collision-induced Rayleigh scattering assumed to be present in liquid chloroform. To close the discussion we point out that Burnham et al [61] have made a detailed study of the internal field corrections available in the literature for light scattering, and point out that for Raman and Rayleigh scattering both the choice of model and the power of the local field correction is in question. The latter point is discussed further by Carlson et al [57]. In order to explain both the observed isotropic intensity and the depolarization ratio simultaneously, it is necessary to use an ellipsoidal model of the internal field. To make any comment on collision-induction from depolarised Rayleigh

intensities, it is necessary to resolve the internal field problem firstly for any molecule whose polarisability tensor has anisotropic components.

Far Infra-red Absorption and Dielectric Relaxation

The far infra-red and dielectric spectrum of liquid chloroform is probably as well studied as that of any other liquid [19,22-27,31,36,43,62-80] both experimentally and theoretically. The entity for analysis is the complete frequency region from zero to THz frequencies. We have already reviewed the work of Gerschel et al (see ref [36] for a summary) along the gas/liquid coexistence line, and ultimately, the computer simulation technique should aim at following these data up to the critical point. The rapid increase in interest in these spectra [19] is justified by their ability to provide information relatively free of the complexities reviewed already in Raman and Rayleigh scattering. The zeroth and second moment of the spectral system are provided routinely through measurements respectively of the dielectric permittivity and power absorption coefficient. Evans et al [81-84] have indicated recently how to make use of fourth and sixth moments available from the accurately known high frequency wing of the far infra-red band when this is free of proper-mode interference. In principle, it is also possible to use the computer to simulate the rotational acceleration correlation functions [84] associated with these high-moment spectra. We need hardly add that a theory should aim to describe all the available spectral moments.

Apart from the substantial shifts in the frequency ($\bar{\nu}_{max}$) of maximum f.i.-r. power absorption observed for the pure liquid by Gerschel [36], the $\bar{\nu}_{max}$ of chloroform shifts with dilution [65, 70] in various non-dipolar solvents. The pure liquid peaks at 36 cm^{-1}, according to Leroy et al. [85], but $\bar{\nu}_{max}$ varies from 25 to 33 cm^{-1} in various solvents. It peaks at 30 cm^{-1} in decalin [43]. These shifts reflect directly the effect of environment on the mean square torque [19, chapter 4]. The dilution studies of Reid et al. [65] reveal clearly that the behaviour of chloroform in carbon

tetrachloride solvent is anomalous in that the frequency shift of $\bar{\nu}_{max}$ with dilution is small, as is the case with Rayleigh scattering [35]. When chloroform is dissolved in decalin and n-pentane $\bar{\nu}_{max}$ shifts from 36 cm^{-1} to 30 cm^{-1} and 25 cm^{-1} respectively; while in carbon tetrachloride $\bar{\nu}_{max}$ seems to increase to 39 cm^{-1}. In diphenylmethane, there is also a small shift to 37 cm^{-1}. It seems therefore that the information obtained from depolarised Rayleigh scattering is restricted by the need to use as solvent the isotropically polarisable CCl_4. Although this solvent is non-dipolar it has a larger (collision-induced) absorption cross-section in the far infra-red than decalin. The far infra-red collision cross-section of diphenyl methane is even larger. (The maximum power absorption for pure liquid decalin, carbon tetrachloride and diphenyl methane is 0.5, 1.8, and 5.5 neper cm^{-1} respectively, the latter having a small dipole moment of 0.6D). The $\bar{\nu}_{max}$ of intensely dipolar solute molecules (such as CH_2Cl_2) shift most on dilution in non-dipolar solvents. In other words, solvent shifts occur when dipolar cross-correlations are reduced by dilution. If the solvent is dipolar, dilution is less effective and the resultant behaviour is more similar to that of the pure liquid solute than it is for a non-dipolar solvent. Therefore in considering far infra-red solvent shifts both the dipolar effect and solvent rotational hindrance effect are contributory factors.

The effect of hydrostatic pressure on the far infra-red spectrum of liquid chloroform shifts the peak to higher frequencies, as shown by Gerschel [36] by heating the liquid in a closed vessel. The effect of supercooling [43] in decalin solvent is also to shift $\bar{\nu}_{max}$ considerably, from 36 cm^{-1} to 50 cm^{-1} in decalin solvent at 110K, and to sharpen the far infra-red (γ) part of the overall (α,β,γ) multi-decalde loss profile [19, chapter 7].

The intensity of the far infra-red band in liquid chloroform has also been studied carefully by a number of groups [43, 73-76]. The integrated intensity of the far infra-red band has been compared with the theoretical

prediction of Gordon's sum rule [86] for the pure liquid by Hindle et al [73] and for a 10% solution in decalin by Reid et al [43], both groups using a simple frequency independent correction for the internal field. Hindle et al find that 88% of the observed intensity is produced by the sum rule, while Reid et al find 73% as an equivalent figure in dilute decalin solution. By making an extensive comparison of the sum rule with far infra-red absorption intensities in other solute/solvent systems Reid et al [43] have come to the conclusion that collision-induced effects are not in the main responsible for the discrepancy between the theoretical and experimental values of integrated absorption intensity.

Bossis [59] has recently discussed the application of the Gordon sum rule to highly dipolar molecules, where a mechanism of dipole-induced dipole induction causes, in principle, the theoretical intensity to be supplemented considerably. He elaborates the original work of Gordon considerably, but comes to the conclusion that induced-effects are unlikely to be important in chloroform liquid, and, according to Gerschel et al. [36], disappear at the critical point. We point out that the contour of the dipole-induced dipole absorption would tend to follow that of the permanent dipole absorption [19, chapter 11]. Quadrupole-induced dipole absorption, on the other hand, would peak at a higher frequency. Therefore it is unlikely that the rotational velocity correlation function of chloroform can be affected, on this evidence, by collisional-induced effects. The strongest evidence against a simple mechanism of collision-induction in chloroform is the linearity of the integrated absorption intensity with dilution.

Assuming, therefore, that the far infra-red band of liquid chloroform is due to reorientation of the permanent dipole moment, several groups have attempted to reproduce the band-shape theoretically [19,43,62-67,69,76,69,83] using modelling techniques based on three-variable Mori theory, the itinerant-oscillator, or constrained-oscillator. Quentrec et al [76] were the first to

develop the Mori continued fraction for use in the complete zero-THz range, and obtained a good fit by regarding their three parameters as variable. Subsequently, this theory has been considerably extended by Grigolini et al [19, chapters 9 and 10], so that an effectively infinite Mori chain can be constructed numerically while keeping the number of phenomenological variables to just one. Reid et al have demonstrated the equivalence of 3 variable Mori theory and the itinerant-oscillator model [43, 65] when the former is applied to angular velocity, and have developed a relation between the mean square torque [81], as estimated from the far infra-red band using this theory, and an independently calculated volume of rotation. Liquid chloroform does not behave anomalously in this respect, while associated liquids such as acetonitrile clearly deviate from the empirical straight line constructed from a combined study of thirty-nine solute molecules in decalin [19, chaper 4].

A recent development in the field of theoretical modelling is the constrained librator model of Gaiduk and Kalmykov [63, 64], which is fitted to liquid chloroform data over the zero-THz range using the minimum of adjustable variables. Evans et al. [70] have also considered theoretically the zero-THz frequency chloroform absorption. All these models contain an element of empiricism, which is transferred to the model of the pair-potential in a computer simulation. A complete analysis would use computer simulation, theory and experimental analysis in combination. In the first instance, we shall aim to see whether the simulation is successful in reproducing the far infra-red bandshape in the pure liquid at 293K, 1bar.

Nuclear Magnetic Resonance Relaxation

Relaxation studies on a variety of nuclei have been reported for liquid chloroform. We have reviewed some of these data already in the section on Rayleigh and Raman scattering. Recently Forsen et al. [87] have discovered pronounced solvent effects on the chlorine magnetic resonance relaxation of liquid chloroform (^{35}Cl and ^{37}Cl nuclei) at 303K. ^{35}Cl transverse relaxation times

are given for the neat liquid and solutions. For neat $CHCl_3$ this is 2.0ps, in 1 : 3 n-hexane it is 1.8ps, and in 1 : 3 CH_2I_2 it is 3.4ps. Shoup et al [88] have measured the ^{13}C spin-lattice (R_1) and spin-spin (R_2) relaxation rates for 60% enriched chloroform. R_1 is dominated by the intra-molecular dipole dipole interaction with the proton, and R_2 by scalar coupling to the chlorine nuclei. The activation energies associated with the anisotropic molecular motion, and rotational diffusion constant were obtained from the ^{13}C relaxation data and found to agree well with those obtained from D and Cl studies by Huntress [89]. Spin-rotation contributions were assumed to be small, and intermolecular contributions to the total spin-lattice relaxation rate (R_1) were not considered, following ref. [90]. R_1 is determined therefore by a correlation time (τ_c) characteristic of the tumbling motion of $CHCl_3$, (as in dielectric relaxation), i.e. motion of the C_{3v} symmetry axis. The ^{13}C - H vector is in this axis and spinning around C_{3v} does not contribute to R_1, which is related to τ_c using the expression involving the dipole-dipole relaxation of two unlike spins 1/2 in the extreme narrowing limit, neglecting cross-relaxation terms, and assuming the model of rotational diffusion [19, chapters 1 and 2] for the molecular dynamics. This gives a correlation time of 1.60ps, which is compared with a value of 1.74ps from ref. [89] (the nuclear D quadrupole relaxation). These are smaller than the transverse relaxation time reported by Forsen et al [87] (2.0ps). Two more values of τ_c are listed by Brodbeck et al [10], namely 1.5ps [34] and 1.73ps [13] at ambient temperature and pressure. A rotating frame spin-lattice relaxation time of 44μs has recently been reported by Ohuchi et al [91], which compared with a ^{35}Cl nuclear quadrupole relaxation time of 21μs in pure $CHCl_3$ reported by Forsen et al [87]. The spin-rotation mechanism is neglected by Shoup et al [88]. The NMR relaxation time reported by Alms et al [34] agrees with the Rayleigh scattering correlation time at infinite dilution. Dinesh et al [92] have also measured the proton spin-

lattice relaxation in liquid chloroform from 219K to 363K at 1bar. According to these authors, the spin-rotational relaxation rate is larger than the intra-molecular dipolar term over the entire temperature range, which conflicts with the view of Shoup et al. [88]. Dinesh et al. also estimate inter-molecular dipolar relaxation rates and report activation energies for the various relaxation mechanisms. Dinesh et al. point out the considerable disagreement in the NMR literature on chloroform prior to the appearance of their paper. This extends to the actual value of the proton spin-lattice relaxation time and to the various contributory factors involved. They write the experimental spin-lattice relaxation rate as a sum of contributions from at least five different sources: intra and intermolecular dipolar mechanisms; spin-rotation; scalar coupling; and the anisotropy of the chemical shift tensor. The first three depend on temperature, the scalar coupling term on temperature and frequency, and the chemical shift tensor on the strength of the magnetic field used. They neglect the last two contributions and from the first three extract a rotational correlation time using rotational diffusion theory. A translational correlation time is also derived, but Dinesh et al. point out that many assumptions are made in data reduction before arriving at this parameter. The rotational correlation time varies from 3.0ps at 219K to 1.39ps at 298K to 1.07ps at 363K; and the translational correlation time from 263ps at 219K to 80.6ps at 298K to 52.2ps at 363K. The rotational correlation times are taken from Huntress [89], and also quoted are diffusion coefficients for tumbling ($D_{\perp}$) and spinning ($D_{\parallel}$) of the $CHCl_3$ molecule. At 298K these are: $D_{\perp} = 1.00 \times 10^{-11} s^{-1}$; $D_{\parallel} = 1.84 \times 10^{-11} s^{-1}$. The anisotropy of the molecular diffusion is much greater at 219K, where $D_{\perp} = 0.38 \times 10^{-11} s^{-1}$ and $D_{\parallel} = 1.20 \times 10^{-11} s^{-1}$. At 293K (computer simulation temp.) Huntress reports [89] $D_{\parallel} = 1.8 \times 10^{-11} s^{-1}$ and $D_{\perp} = 0.96 \times 10^{-11} s^{-1}$, which provide correlation times for tumbling and spinning of 1.8ps and 0.92ps respectively, but for $CDCL_3$, and not $CHCl_3$. In table 1 we compare these values directly with the results of

our computer simulation. Therefore the results of Huntress indicate that motion about the symmetry axis is faster by a factor of about two, at 293K, 1bar, than the motion about a perpendicular axis. In contrast, in the gas phase, $CDCl_3$ rotates about twice as fast about a perpendicular axis as it rotates about the C_{3v} axis. This conflicts with the data of Forsen et al. [87] on ^{35}Cl transverse relaxation times. The liquid phase behaviour may be attributable, according to Huntress, to weak H-bonding, or self-association. This may be tested by computer simulation, where we do not allow for H-bonding.

Farrar et al [93] report the temperature dependence of ^{13}C relaxation studies in $CHCl_3$, but do not reduce their data directly to correlation times. Duplan et al [94] report the Overhauser effect on the ^{13}C - ^{1}H nuclei in chloroform, providing a relaxation time of 1.26 $\pm$ 0.04ps for the motion of an axis perpendicular to the C - H axis, i.e. this is the second-rank orientational correlation time of the C_{3v} axis tumbling in $CHCl_3$ - the dipole axis. This compares with an equivalent value of 1.8ps from Huntress [89]; 1.6ps [88]; 1.5ps [34] and 1.7ps [13] from other sources in the literature.

In summary, therefore, the various NMR methods can provide us in principle with valuable data on the anisotropy of rotational diffusion in chloroform, but the various assumptions involved in the data reduction reduce the absolute validity of the final correlation times obtained. There seems to be conflicting evidence as regards anisotropy of the motion of $CHCl_3$ molecules in the liquid.

Non-Linear Techniques

The Kerr effect in liquid chloroform has been studied experimentally and theoretically by several groups [95-104]. Ho et al [100] and Ratzch et al. [99] have pioneered the electrooptical Kerr effect, where liquid phase anisotropy is induced by electromagnetic radiation, enabling the use of experiments on a picosecond time-scale with trains of laser pulses. Perhaps the most careful measurements on the conventional (electric field-induced) Kerr effect are those reported by Beevers et al [95, 96] for a number of liquids, including chloroform,

over the temperature range 175 to 343K. The Kerr effect, according to Beevers et al, is a sensitive probe of liquid structure, and is related to the polarization $\langle P_1(\cos\Theta)\rangle_E$ and alignment $\langle P_2(\cos\Theta)\rangle_E$ where P_1 and P_2 are the first and second Legendre polynomials, respectively, and Θ is the angle between the dipole axis of the reference molecule and the applied field. For axially symmetric molecules such as chloroform and acetonitrile, Kerr effect, dielectric, and light scattering data are combined to analyse the temperature dependence [95] of $\langle P_2(\cos\Theta)\rangle_E$ to obtain information about two and three particle correlation fuctions. The Kerr effect, apart from computer simulation, is an almost unique source of information concerning three particle correlations. $\langle P_1(\cos\Theta)\rangle_E$ and $\langle P_2(\cos\Theta)\rangle_E$ occur directly in two other related experiments [105], dielectric polarisation [102] and from the effect of an applied electric field on NMR relaxation. By combining dielectric permittivity and Kerr effect data, Beevers et al calculate $\langle P_2(\cos\Theta)\rangle_E$ and compare it with the result obtained from the electric N.M.R. experiment. Buckingham [106] has proposed that a study of $\langle P_1(\cos\Theta)\rangle_E$ and $\langle P_2(\cos\Theta)\rangle_E$ would test the validity of the effective field approximation [19, chapter 3]. Beevers et al [95] place chloroform in the category of molecular liquids where there is no hydrogen-bonding of significance, and where orientational order is dominated by shape and electrodynamic effect, as in our computer simulation.

Beevers et al provide values for the correlation parameters g_1, g_2 and g_3, defined by:

$$g_1 = 1 + \sum_{i\neq 1} \langle \cos\Theta_{1i} \rangle$$

$$g_2 = 1 + \sum_{i\neq 1} \langle \frac{3}{2}\cos^2\Theta_{1i} - \frac{1}{2} \rangle$$

$$g_3 = 1 + \sum_{i\neq 1} \sum_{i\neq 1\neq j} \langle \frac{3}{2}\cos\Theta_{1i}\cos\Theta_{1j} - \frac{1}{2}\cos\Theta_{ij} \rangle$$

where Θ in these equations is the angle between the axis of neighbouring dipoles, the summation extending over all molecules correlated to a

reference molecule, and the statistical averages taken in the absence of an applied field. g_1 is the Kirkwood correlation parameter of the Kirkwood-Frohlich equation [19, chapter 3] and g_2 is determined from a comparison of Rayleigh and "single-particle" (N.M.R. or Raman) correlation times. A combination of techniques [95] yields g_3. For liquid chloroform at 293K, Beevers et al provide $g_1 = 1.4$, $g_2 = 1.7$, and $g_3 = -0.40$. g_1 remains constant with temperature but g_2 and g_3 show a weak temperature dependence. Gerschel et al [27] also found that g_1 was independent of temperature and deduced a value of about 1.25 from the static permittivity, while Rosenthal et al [40] obtained $g_1 = 1.32$ from the far infra-red. Beevers et al remark that it is not clear why g_1 is independent and g_2 and g_3 dependent on temperature. g_3 is significantly different when calculated according to refs [105] or [107]. In principle, it is possible to obtain g_1, g_2 g_3 by computer simulation, but with a bigger sample of molecules than used in this work to minimize the effect of periodic boundary conditions.

Beevers et al mention some of the theoretical difficulties of reducing Kerr effect data, primarily the problem revolves around that of the internal field effect [19]. Proutiere et al. [97] have compared some experimental results obtained for liquid chloroform with the Kerr effect with those obtained from other sources. These include induced birefringence and depolarised Rayleigh scattering. They show that the theoretical expression of Langevin/Born is not valid in condensed media. They make a critical study of this equation for the Kerr constant with results concerning the evaluation of orientational molecular energy, non-linear optical phenomena, molecular correlations and interactions, electrostriction, and Joule's effect. An improved theoretical expression for the Kerr constant is proposed and applied to experimental data. Proutiere et al. point out that in the static Kerr effect, the applied field is strong, so that it is necessary to take account of non-linear polarisation phenomena, as described by Beevers et al. Buckingham et al

[108] have shown that hyperpolarisability effects are discernable in the Kerr effect applied to gases. Proutiere et al. [97] list some values of the second-order hyperpolarisability obtained from the Kerr effect, but not for $CHCl_3$. They also agree with Beevers et al that angular correlations must be accounted for correctly in the Kerr effect, and discuss the influence of electrostriction, which is, theoretically, [107, 109] an isotropic effect related to the change of volume on application of an electric field to a liquid. Similarly, the Joule effect seem to have no influence on their Kerr constants.

Burnham et al. [101] have recently used results from the optical Kerr effect, Cotton-Mouton effect and light scattering to obtain orientational pair correlation functions for liquid chloroform from the theory of Ladanyi and Keyes [110]. Orientational pair correlation parameters for liquid acetone were obtained having values ranging from (anisotropic Rayleigh scattering) to (Kerr effect). The non-linear refractive index of liquid chloroform has been derived for the first time by Ho et al [100] using the optical Kerr effect induced by picosecond laser pulses. This factor contains all the non-linear contributions from electronic, librational and reorientational motions, and this technique is potentially of great interest.

Brillouin Scattering and Sound Dispersion

These techniques can be used in combination to provide information on density fluctuations and vibration/translation coupling [111-118]. Takagi et al [115] have made ultrasonic measurements in liquid chloroform over the frequency range from 3 MHz to 5GHz using pulse-echo overlap, high-resolution Bragg reflection and Brillouin scattering. The observed velocity dispersion revealed two relaxation processes, one at 650 MHz and the other at 5.1 GHz at 293K. The lowest (261 cm^{-1}) and second lowest (366 cm^{-1}) fundamental vibrational modes have a common relaxation time at 50 ps. Everything above the third mode (667 cm^{-1}) at 290 ps. These compare with a relaxation time of 104 ps measured by Samios et al [111] for sound wave relaxation.

Yoshihara et al [118] have measured the refractive indices and Brillouin frequencies for chloroform. The hypersonic velocity data show significant deviations from the law of corresponding states. Altenberg [116] has discovered that the sound velocities of a number of organic compounds, including chloroform, is smaller in the deuterated analogue. Sarnios et al [111] measured the temperature dependence of the relaxation strength, which is an indication of the nature of the observed relaxation process. Translation/vibration energy transfer is observed, involving the lowest and second-lowest energy level. The temperature dependence of the relaxation time provides information on the inelastic collision cross-section and on the nature of the intermolecular potential. Vallauri et al. [117] have also analysed the temperature variation of the relaxation time in liquid chloroform, which is described as "non-associated". This is achieved by means of the frequency shift of the Brillouin peak as a function of the temperature, which provides direct information on the mean energy exchanged in a single collision and on the minimum approach distance in the trajectories of two colliding chloroform molecules.

In overall summary, therefore, over a hundred papers have appeared in the last decade on various structural and dynamical aspects of liquid chloroform and its isotopic analogues. The problem is to explain this mass of data consistently, preferably using no adjustable parameters. A considerable amount of the available experimental data is contradictory or restricted in scope, so that some point of reference is needed with which to compare the experimental results and trends. Particularly, confusion exists about the role of collision-induced scattering, the nature of the internal field, rotation-vibration coupling, vibrational cross-correlation, and anisotropy of diffusion in liquid chloroform. The NMR relaxation data seem to provide two different and irreconcilable conclusions about whether the chloroform molecule (or $CDCl_3$)

spins faster than it tumbles. Chloroform liquid has been characterised perhaps with most certainty in the dielectric and far infra-red range of frequencies, and there is evidence from various sources to suggest that the role of collision-induced absorption is a minor one in this frequency range.

All this points towards the necessity for a coordinated look at liquid chloroform over a much wider range of conditions than hitherto reported, and towards a simulation by computer under well defined conditions.

Computer Simulation Methods and Results

The basic algorithm, TETRAH, was obtained from the SERC CCP5 library and modified considerably by Ferrario et al. [119]. Subsequently, computer simulations have been carried out on a variety of molecules but keeping to the same atom-atom Lennard-Jones parameters, so that, eventually, a consistent picture will begin to emerge from different simulation/data comparison exercises.

TETRAH was modified to involve charge-charge interaction and a force cut-off criterion based on centre of mass to centre of mass distance (cut off radius = 12.2Å). The equations of translational motion were solved with a third order predictor routine and those of rotational motion using as coordinates the angular momentum and the three unit vectors along the principal axes of the moment of inertia tensor. The Lennard-Jones parameters are: $\sigma(H - H) = 2.75$Å; $\sigma(Cl - Cl) = 3.50$Å; $\sigma(C - C) = 3.20$Å; $\varepsilon/k\ (H - H) = 13.4$K; $\varepsilon/k(Cl - Cl) = 175$K; $\varepsilon/k(C - C) = 51.0$K [120]. Partial charges were added to each atomic site [120] of $q_H = 0.131|e|$; $q_C = 0.056|e|$; $q_{Cl} = -0.063|e|$.

The simulation was carried out with input parameters corresponding to the molar volume of liquid chloroform at 293K, 1 bar, using 108 molecules which were arranged initially on a face-centred cubic lattice. After equilibration, dynamical data were sampled at time intervals of 5×10^{-15} s, and stored on disk. Atom-atom p.d.f.'s were computed over some 10,000 time steps, and auto-correlation functions computed with subsidiary algorithms using running-time averages [19].

The algorithm produces equilibrium properties in the course of a run. The pressure being a difference of two large numbers, fluctuates considerably more than any other quantity in a molecular dynamics simulation, and is extremely sensitive to small changes in the pair-potential. These are reported in ref. [120], the output pressure fluctuates by about 300bar about 1 bar.

Atom-Atom Pair Distribution Functions

These are compared with the results of Bertagnolli [1] in figs (1) to (3). In fig. (1) the overall structure of the experimentally derived and simulated carbon to carbon p.d.f. is similar, although detailed agreement

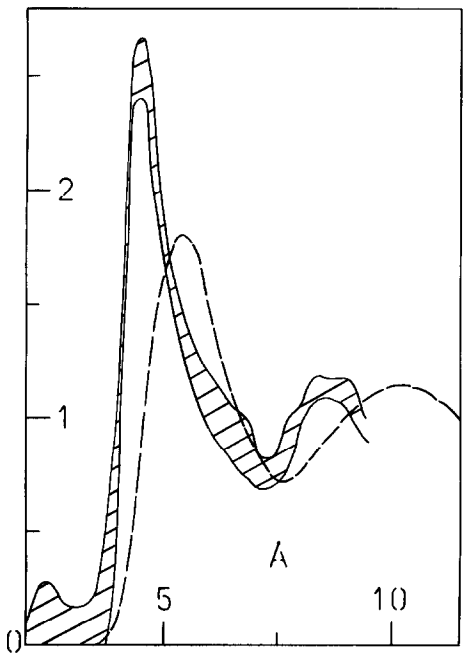

Figure (1)

Carbon-carbon probability density functions for chloroform at 293K, 1bar.

////// Neutron diffraction [1].

- - - Computer simulation.

is not obtained. The experimental results in fig. (1) seem to indicate that the chloroform structure is slightly more tightly packed than the simulation parameters allow for. This picture is not corroborated in figs (2) and (3), however, because the position of the first peaks in the experimental and numerical data agree closely. Thereafter, however, the two sources are less

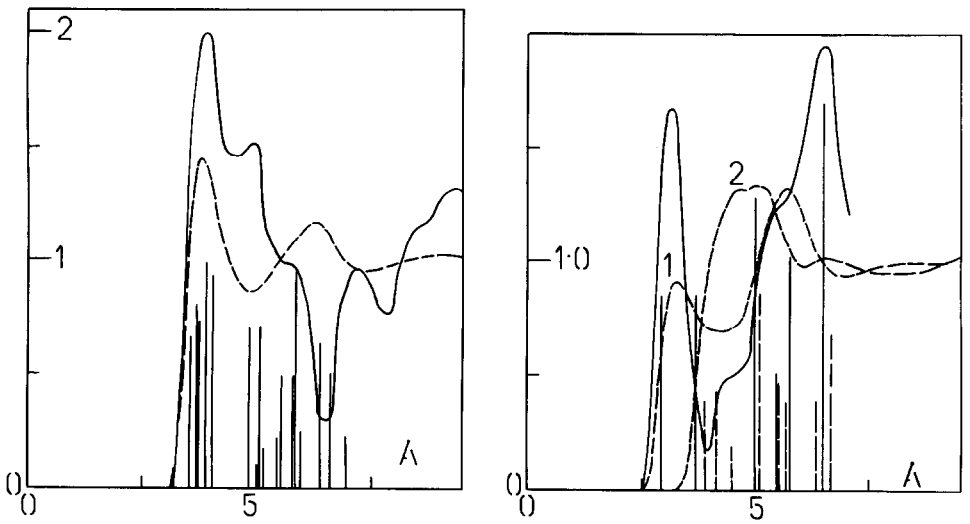

Figure (2)

Chlorine-chlorine p.d.f.

——— Neutron diffraction [1].

- - - Simulation

| Crystal data [1].

Figure (3)

——— Sum of Cl - H and Cl - C p.d.f.'s [1].

- - - (1) Simulation (Cl - H)

- - - (2) Simulation (Cl - C)

| (Double scale), Cl - H, crystal data [1]

| (Single scale), Cl - C, crystal data [1]
|

consistent. It is noticeable, however, that the simulated p.d.f.'s tend to be broadened out versions of the delta functions in figs (2) and (3) obtained from crystal data [1]. Judging by the noise level of the experimental data in fig. (1), those of figs (2) and (3), being combinations of as many as four or five noisy functions such as that of fig. (1), must be viewed with caution. The experimentally derived curve in fig. (3) is a sum of the Cl to H and Cl to C atom-atom p.d.f.'s. The simulation provides these separately. The position of the first peak in fig. (3) is consistently established, and possibly that at 5.5Å, but otherwise detailed agreement is not obtained. Again the simulated p.d.f.'s tend to be broadened versions of the crystalline data. The other two atom-atom p.d.f.'s simulated in this work have been reported in ref. [120]. As the first comparison of its kind, this one may be summarized as resulting broadly in agreement, but establishing that the noise level in the experimental p.d.f.'s is rather too high for detailed comment beyond the first peak in each p.d.f., with the exception of the carbon-carbon function.

Dynamical Data

A great deal of the available spectral data may be compared conveniently with a few reference autocorrelation functions from the computer simulation. The Raman and Rayleigh scattering correlation times may be compared with the second rank reorientational auto-correlation times for spinning and tumbling (table 1), and the infra-red and dielectric correlation times with the first rank orientational a.c.f.'s from the computer simulation. Similarly, the various N.M.R. times can be matched with the second rank orientational times. A preliminary comparsion of this kind has been reported in ref. [120]. Table (1), however, is a much fuller synopsis of the available data. The correlation times from the computer simulation are defined as the areas beneath the respective correlation functions, illustrated elsewhere [120].

By comparing the reorientational a.c.f.'s of $\underline{e}_3$ (a unit vector in the C_{3v} axis) and $\underline{e}_1$ (a unit vector in a perpendicular axis through the centre

of mass) the simulation suggests that the anisotropy of the rotational diffusion is smaller than that of Huntress [89] and in the opposite sense. That is to say, the spinning motion, characterised by $\langle \underline{e}_1(t).\underline{e}_1(o)\rangle$, has a longer correlation time than the tumbling, characterised by $\langle \underline{e}_3(t).\underline{e}_3(o)\rangle$. This is the "gas-phase" result [89], and is the result suggested by Forsen et al [87] from ^{35}Cl measurements. It is also interesting to note that the Raman correlation times for the totally symmetric C-Cl band ($\nu_3(A_1)$) listed by Brodbeck et al [10] are longer than those from the $\nu_1(A_1)$ and $\nu_2(A_1)$ modes, which again means that spinning is slower than tumbling, not faster than tumbling as suggested by Huntress. The first (τ_1) and second (τ_2) rank reorientational autocorrelation times from the computer simulation are: $\tau_1(\underline{e}_1)$ = 3.9ps; $\tau_2(\underline{e}_1)$ = 1.5ps; $\tau_1(\underline{e}_3)$ = 3.6ps; $\tau_2(\underline{e}_3)$ = 1.3ps. The first rank autocorrelation functions become exponential after about 1 ps, but the second rank a.c.f.'s are not so up to about 2.5ps. Since there are "single-particle", or auto, correlation functions they are not directly comparable with dielectric relaxation times, which contain cross-correlations between different molecules [19]. The dielectric relaxation work on chloroform in various solvents over the last decade has been summarised conveniently by Akhadov [121]. Chloroform has been studied dielectrically in about fifty different solvents, dipolar and non-dipolar. Some of the available dielectric relaxation times are summarised in table 1. Kluk et al [31] have recently made a careful study over a range of temperature for the pure liquid. At 293K, Akhadov lists a number of estimates of the dielectric relaxation time (τ_D). In the pure liquid at 293K, τ_D = 6.2ps [ref. 121, p.219]; τ_D = 4.7ps [ref. 121, p. 220]; τ_D = 6.0ps [ref. 121, p. 221]. These relaxation times fall considerably on dilution. We have 3.2ps in cyclohexane [ref. 121, p. 221, ref. 122], 4.3 $\pm$ 0.3ps in decalin [43] and 5.0ps in CCl_4 [122]. These compare with a computer simulated auto-correlation time of 3.5ps. There is a surprisingly large spread of uncertainty in the available experimental

data, but it is clear that the experimental correlation times (involving cross-correlations) cluster around a value for the pure liquid which is longer than the simulated correlation time. In dilute solution in decalin [43] or cyclohexane [121], the simulated and measured correlation times overlap, suggesting a reduction in cross-correlations. The dielectric measurements of Kluk et al [31] show that the dielectric relaxation time varies from 6.0ps at 293K to 17.0ps at 223K. These authors develop a theory to relate the dielectric relaxation time to the single particle correlation time produced by computer simulation. The Kirdwood factor is very nearly one, according to Kluk et al [31]. This conclusion is based on freshly measured dielectric and Raman correlation times over a wide temperature range. Evans [120] has attempted to compute orientational cross-correlation functions for liquid chloroform using small sub-spheres of two or three particles in the computer simulation with 108 molecules. The computed orientational a.c.f.'s and these microscopic sub-sphere correlation functions behave similarly. A bigger sample is needed in order to assess these effects more accurately by computer simulation. The available correlation times are summarised in table (1).

The far infra-red spectrum is the high frequency adjunct [19] of the dielectric loss, and may be related via a Fourier transform to the rotational velocity a.c.f. [26]: $\langle \dot{\underline{e}}_3(t).\dot{\underline{e}}_3(o)\rangle$. This is illustrated in ref. [120], and is similar in shape to the orthogonal r.v.c.f. $\langle \dot{\underline{e}}_1(t).\dot{\underline{e}}_1(o)\rangle$ indicating that the anisotropy of the diffusion at short times is small. The Fourier transform of $\langle \dot{\underline{e}}_3(t).\dot{\underline{e}}_3(o)\rangle$ peaks at $31cm^{-1}$, which compares with an experimental value of 36 cm^{-1} in the pure liquid, and 30 cm^{-1} in cyclohexane [65]. The shapes of the simulated and experimental curves are similar, both in the frequency and time domains [19, chapter 4], so that collision induced absorption and hydrogen-bonding effects do not seem to be important in the far infra-red for liquid chloroform. In other liquids [43, 19] the effects of association are pronounced. The simulated far infra-red maximum absorption frequency ($\bar{\nu}_{max}$)

of 31 cm^{-1} is lower than the observed $\bar{\nu}_{max}$ of 36 cm^{-1} [65]. These two results are not directly comparable, however, because the computer simulation refers to autocorrelations only. The experimental spectrum, on the other hand, is the result of the interaction with the molecular ensemble of electromagnetic radiation. The field strength of this radiation at a given molecule in the ensemble is not the same as that outside the macroscopic sample because of the polarisation of its surroundings by the molecular electric field [19, chapter 3]. The degree of polarisation varies with the angular and linear momentum of the molecule and is therefore frequency dependent. A frequency dependent correction has to be applied to the experimental spectral intensity (e.g. power absorption coefficient) to account for this so-called "dynamic internal-field effect". After this correction has been applied, the resulting bandshape may be related to a correlation function assuming the validity of the fluctuation - dissipation theorem [19, chapter 1-3] in the adiabatic approximation. The internal field correction is dependent on the shape of the dielectric under consideration, on cavity theory [19, chapter 3], and various other sample assumptions. Allowing for these, the rotational velocity correlation function obtained from an internal-field corrected Fourier transform of the far infra-red power absorption coefficient, $\alpha(\bar{\nu})$, is a cross-correlation function in the pure liquid. Chatzidimitriou-Dreismann et al [123-125] have recently questioned the basic validity of the adiabatic approximation in fundamental fluctuation-dissipation theory, following the criticisms of Kubo's analysis [126] by van Vliet [127, 128] and van Kampen [129]. The use of non-adiabatic fluctuation-disspation theory opens up a range of fascinating possibilities, especially regarding spectral moment analysis [19, chapter 1; 81-84] because several of the "symmetry theorems" on the fundamental properties of auto-correlation functions and spectral moments [19] are valid only in the adiabatic approximation. The possibilities are especially exciting in the far infra-red [123-125].

We note that fluctuation-dissipation theory is not necessary for the construction of an auto-correlation function in a computer simulation because we are not perturbing the sample in any way with probe radiation in order to see into its dynamical behaviour. The role of non-adiabatic corrections to fluctutation-dissipation theory may therefore be discerned by comparing the simulation with far infra-red spectral data in combination with dielectric data (i.e. using both available spectral moments).

The overall conclusion (fig. (4)), from the comparison of the simulated far infra-red band-shape with the data is that the latter may be approximated with autocorrelations. The shapes of the two curves are similar, so that collision-

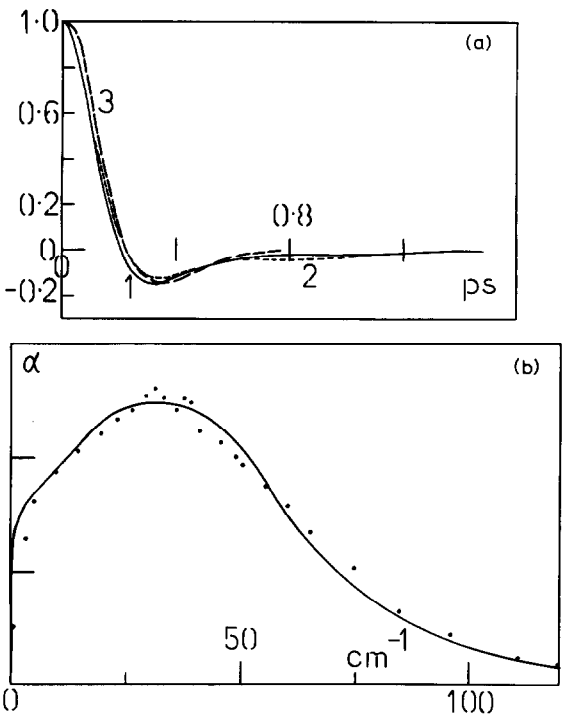

Figure (4)

Comparison of simulated [120] and experimental [26] r.v.c.f.'s for $CHCl_3$.
(1) Simulation; (2) measured and corrected [26] for induced absorption.

induced distortion, internal-field effects, cross-correlations, hydrogen-bonding effects, and non adiabatic corrections seem to be small. The exercise should be repeated at state points under hydrostatic pressure and to the critical point. The computer simulation has not been used to provide an accurate assessment of the intensity of the far infra-red spectrum, but, rather, of the shape and position of the spectrum. These agree satisfactorily with the data given all the assumptions involved.

Fundamental Molecular Dynamics in Liquid Chloroform

Having assessed the validity of the molecular dynamics method with the available data we can use the numerical data to probe the nature of the molecular dynamics at a fundamental level. The details of this investigation are reported elsewhere [120], one of the major conclusions being that the probability density functions [19] governing the approach to equilibrium are not Gaussian. The rotation of a chloroform molecule is statistically correlated with its centre of mass translation. This may be discerned in a frame of reference which rotates with the chloroform molecule by constructing the correlation matrix $\langle \underline{v}(t)\underline{J}^{T}(o)\rangle$ in this frame. There is no analytical theory available yet to describe this result, even in an approximate way.

The simulation method throws up a number of new problems which cannot be approached with the classical (purely rotational) theory of molecular diffusion, based on Langevin or Fokker-Planck equations [19]. Perhaps the most promising line of approach to these new phenomena is to involve in the basic Fokker-Planck structure a superimposed potential term, which transforms the Fokker-Planck equation into a Kramers equation [19, chapters 2, 9 and 10]. Grigolini et al [130;141] have recently developed powerful numerical methods to solve the Kramers equation through an adiabatic elimination procedure (AEP) and continued fraction procedure (CFP) which effectively takes the Mori continued fraction to infinity [19, chapters 9 and 10]. These methods have a number of fields of application (outside the area of molecular dynamics

simulation) which have in common the need to solve Kramers diffusion equations of specific types. It is likely, therefore, that theoretical methods developed to deal with new problems from computer simulation will be useful in other fields and vice-versa.

Acknowledgements

The SERC CCP5 group is acknowledged for the basic algorithm TETRAH, and SERC is thanked for the award of an A.F. Dr. M. Ferrario is thanked for many useful suggestions as to the implementation of modified TETRAH.

References

1. H. Bertagnolli, Ber. Buns. Phys. Chem, 85 (1981) 644.
2. O. Steinhauser and H. Bertagnolli, Ber. Buns. Phys. Chem., 85 (1981) 45.
3. H. Bertagnolli and M. D. Zeidler, Mol. Phys., 35 (1978) 177.
4. H. Bertagnolli and P. Chieux, Ber. Buns. Phys. Chem., 84 (1980) 1225.
5. H. Bertagnolli, D. O. Leicht, M. D. Zeidler and P. Chieux, Mol. Phys., 36 (1978) 1769; 35 (1978) 199.
6. H. Bertagnolli, D. O. Leicht and M. D. Zeidler, Mol. Phys., 35 (1978) 193.
7. C. Hoheisel and M. D. Zeidler, Ber. Buns. Phys. Chem., 83 (1979) 28.
8. D. A. McQuarrie, "Statistical Mechanis", Harper and Row, N.Y., 1976, p. 315.
9. C. Hoheisel and U. Deiters, Ber. Buns. Phys. Chem., 81 (1977) 1225.
10. C. Brodbeck, I. Rossi, Nguyen Van Thanh and A. Ruoff, Mol. Phys., 32 (1976) 71.
11. F. J. Bartoli and T. A. Litovitz, J. Chem. Phys., 56 (1972) 413.
12. P. van Konynenberg and W. A. Steele, J. Chem. Phys., 56 (1972) 4776.
13. J. H. Campbell and J. Jones, Chem. Phys. Lett; 18 (1973) 441.
14. J. Soussen-Jacob, E. Dervil, and J. Vincent-Geisse, Mol. Phys., 28 (1974) 935.
15. A. E. Boldeskul, S. S. Esman and V. E. Pogorelov, Opt. Spectrosk., 37 (1974) 521.

16. D. A. Wright and M. T. Rogers, J. Chem. Phys., 63 (1975) 909.

17. A. M. Amorim da Costa, M. A. Norman and J. H. R. Clarke, Mol. Phys., 29 (1975) 191.

18. G. D. Patterson and J. E. Griffiths, J. Chem. Phys., 63 (1975) 2406.

19. M. W. Evans, G. J. Evans, W. T. Coffey and P. Grigolini, "Molecular Dynamics and Theory of Broad Band Spectroscopy", Wiley/Interscience, N.Y., 1982, chapter 1.

20. S. Bratos, J. Rios and Y. Guissani, J. Chem. Phys., 52 (1970) 439.

21. S. Bratos and E. Marechal, Phys. Rev., 4 (1971) 1078.

22. A. Gerschel, 1971, These, Univ. de Paris XI.

23. R. Fauquembergue, 1968, These de 3e cycle, Lille.

24. J. L. Greffe, J. Goulon, J. Brondeau, and J. L. Rivail, J. de Chim. Phys., 70 (1973) 282.

25. A. Gerschel, Ber. Buns. Phys. Chem., 76 (1972) 254.

26. A. Gerschel, I. Darmon and C. Brot, Mol. Phys., 23 (1972) 317.

27. A. Gerschel and C. Brot, Mol. Phys., 20 (1971) 279.

28. J. Schroeder, V. H. Schiemann and J. Jonas, Mol. Phys., 34 (1977) 1501.

29. J. Schröder and J. Jonas, Chem. Phys., 34 (1978) 11.

30. J. Schröder, V. H. Schiemann and J. Jonas, J. Chem. Phys., 69 (1978) 5479.

31. M. W. Evans, M. Ferrario, B. Janik and E. Kluk, Chem. Phys., in press.

32. P. A. Lund, O. Faurskov-Nielsen and E. Praestgaard, Chem Phys., 28 (1978) 167.

33. S. Claesson and D. R. Jones, Chem. Scripta, 9 (1976) 103.

34. G. R. Alms, D. R. Bauer, J. I. Brauman and R. Pecora, J. Chem. Phys., 59 (1973) 5310.

35. K. Kamogawa, Bull. Chem. Soc. Japan, 51 (1978) 3475.

36. A. Gerschel, J. Chim. Phys., Phys. Chim, Biol., 75 (1978) 97.

37. T. Suzuki, Y. K. Tsutsui and T. Fujiyama, Bull. Chem. Soc. Japan, 53 (1980) 1931.

38. G. C. Pimentel and A. L. McClellan, "The Hydrogen Bond", W. H. Freeman and Co., San Francisco (1960).

39. W. G. Rothschiled, G. J. Rosasco and R. C. Livingston, J. Chem, Phys., 62 (1975) 1253.

40. L. C. Rosenthal and H. L.Strauss, J. Chem. Phys., 64 (1976) 282.

41. A. Moradi-Araghi and M. Schwartz, J. Chem. Phys., 68 (1978) 5548.

42. P. C. M. van Woerkom, J. de Bleijser, M. de Zwart, P. M. J. Burgers and J. C. Leyte, Ber. Buns. Phys. Chem., 78 (1974) 1303.

43. C. J. Reid and M. W. Evans, Mol. Phys., 40 (1980) 1357.

44. K. Tanabe and J. Hiraishi, Chem. Phys. Letters, 71 (1980) 460.

45. A. Laubereau, G. Wochner and W. Kaiser, Chem. Phys., 28 (1978) 363.

46. A. Laubereau, C. R. Int. Conf. Sp. Raman 7th, (1980), p. 450.

47. A. Laubereau, S. F. Fischer, K. Spanner and W. Kaiser, Chem. Phys., 31 (1978) 335.

48. A. Moradi-Araghi and M. Schwartz, J. Chem. Phys., 71 (1979) 166.

49. W. G. Rothschild, J. Chem. Phys., 65 (1976) 455.

50. R. K. Wertheimer, Mol. Phys., 36 (1978) 1631; 35 (1978) 257.

51. S. R. J. Brueck, Chem. Phys. Lett., 50 (1977) 516.

52. R. G. Gordon, J. Chem. Phys., 42 (1965) 3658.

53. A. van der Avoird, P. E. S. Wormer, F. Mulder, and R. M. Berns, in "Topics in Current Chemistry", Voo. 93, ed. Dewar et al., Springer-Verlag, 1980.

54. J. Yarwood, R. Arndt and G. Döge, Chem. Phys., 25 (1977) 387.

55. D. W. Oxtoby, D. Levesque and J.-J. Weis, J. Chem. Phys., 68 (1978) 5528.

56. G. Doege, T. Bien and M. Possiel, Ber. Buns. Phys. Chem., 85 (1981) 1074.

57. C. W. Carlson and P. J. Flory, J. Chem. Soc., Faraday Trans. II, 73 (1977) 1729.

58. J. A. Bucaro and T. A. Litovitz, J. Chem. Phys., 54 (1971) 3846; 55 (1971) 3585.

59. G. Bossis, These d'etat, Univ, de Nice, 1981.

60. J. H. K. Ho and G. C. Tabisz, Can. J. Phys., 51 (1973) 2025.

61. A. K. Burnham, G. Alms and W. H. Flygare, J. Chem, Phys., 62 (1975) 3289.

62. H. J. Arning, K. Tibulski and T. Dorfmuller, Ber. Buns. Phys. Chem., 85 (1981) 1068.

63. V. I. Gaiduk and Y. P. Kalmykov, J. Chem. Soc., Faraday Trans. II, 77 (1981) 929.

64. Y. P. Kalmykov and V. I. Gaiduk, Z. Fis. Khim., 55 (1981) 305.

65. C. J. Reid and M. W. Evans, Spectrochim. Acta, 36A (1980) 733.

66. C. J. Reid and M. W. Evans, J. Chem. Soc., Faraday Trans. II, 76 (1980) 286.

67. S. Ikawa, K. Sato and M. Kimura, Chem. Phys., 47 (1980) 65.

68. K. Sato, Y. Ohkubo, T. Moritsu, S. Ikawa, and M. Kimura, Bull, Chem. Soc. Japan, 51 (1978) 2493.

69. F. Hermans and E. Kestemont, Chem. Phys. Letters, 55 (1978) 305.

70. G. J. Evans, Spectrochim. Acta, 33A (1977) 699.

71. J.-L. Greffe and C. Gross, J. Chim, Phys., Phys. Chim. Biol., 75 (1978) 127.

72. J. S. Anderson, W. E. Vaughan, L. C. Rosenthal and H. L. Strauss, J. Chem. Phys., 65 (1976) 2481.

73. P. Hindle, S. Walker, and J. Warren, J. Chem. Phys., 62 (1975) 3230.

74. M. N. Afsar, J. B. Hasted, M. S. Zafar and G. Chantry, Chem. Phys. Letters, 36 (1975) 69.

75. M. Benson, G. D. Martin, S. Walker and R. Wilson, Can. J. Chem., 50 (1972) 2610.

76. B. Quentrec and P. Bezot, Mol. Phys., 27 (1974) 879.

77. A. M. Evseev, and A. F. Lemberskii, Dokl. Akad. Nauk, SSSR, 219 (1974) 126.

78. J. L. Greefe, J. Goulon, J. Brondeau, and J.-L. Rivail, J. Chim, Phys. Chim. Biol., 70 (1973) 282.

79. R. Lobo, J. E. Robinson and S. Rodriguez, J. Chem. Phys., 59 (1973) 5992.

80. J. Goulon, J. -L. Rivail, J. W. Fleming, J. Chamberlain and G. Chantry, Chem. Phys. Letters, 18 (1973) 211.

81. M. W. Evans, J. Chem. Phys., 77 (1982) 108.

82. M. Veerappa, G. J. Davies and M. W. Evans, Chem. Phys., 61 (1981) 73.

83. M. W. Evans, G. J. Evans and B. Janik, Specrochim. Acta, 38A (1982) 423.

84. M. W. Evans, Chem. Phys., 62 (1981) 481.

85. Y. Leroy, E. Constant, C. Abbar and P. Desplanques, Adv. Mol. Rel, Proc., 1 (1967) 273.

86. R. G. Gordon, J. Chem. Phys., 38 (1963) 1724.

87. S. Forsen, H. Gustavsson, B. Lindman and N.-O. Persson, J. Mag. Res., 23 (1976) 515.

88. R. R. Shoup and T. C. Farror, J. Mag. Res., 7 (1072) 48.

89. W. T. Huntress, J. Phys. Chem., 73 (1969) 103.

90. K. F. Kuhlmann, D. M. Grant, and R. K. Harris, J. Chem. Phys., 52 (1970) 3439.

91. M. Ohuchi, T. Fujito and M. Imanari, J. Mag. Res., 35 (1979) 415.

92. Dinesh and M. T. Rogers, J. Chem. Phys., 56 (1972); Chem. Phys. Letters, 12 (1971) 352.

93. T. C. Farrar, S. J. Druck, R. R. Shoup and E. D. Becker, J. Am. Chem. Soc., 94 (1972) 699.

94. J. C. Duplan, A. Briguet, and J. Delmar, J. Chem. Phys., 59 (1973) 6269.

95. M. S. Beevers and G. Khanarian, Aust. J. Chem., 33 (1980) 2585.

96. M. S. Beevers and G. Khanarian, Aust. J. Chem., 32 (1979) 263.

97. A. Proutiere and J. G. Baudet, Ann. Univ. Abidjan, Ser. C, 11 (1975) 13.

98. S. Wozniak and S. Kielich, J. Phys. (Paris), 36 (1975) 1305.

99. M. T. Ratzch, E. Rickelt and H. Rosner, Z. Phys. Chem., 256 ((1975) 349.

100. P. P. Ho and R. R. Alfano, Phys. Rev., 20 (1979) 2170.

101. A. K. Burnham and T. D. Gierke, J. Chem. Phys., 73 (1980) 4822.

102. V. I. Slipchenko, Ukr. Fiz. Zh., 26 (1981) 147.

103. K. J. Witte, M. Galanti and R. Volk, Opt. Comm., 34 (1980) 278.

104. W. H. Nelson, J. Chem. Phys., 76 (1972) 1502.

105. J. D. Ramshaw, D. W. Schaefer, J. S. Waugh, and J. M. Deutch, J. Chem. Phys., 54 (1971) 1239.

106. A. D. Buckingham, Chem. Br., 1 (1965) 54.

107. A. D. Buckingham and B. J. Orr, Trans. Faraday Soc., 65 (1969) 673;
108. M. P. Bogaard, A. D. Buckingham and G. L. D. Ritchie, Mol. Phys., 18 (1970) 575.

109. S. Kielich, Acta Phys. Polonica, 4 (1966) 683.

110. B. M. Ladanyi and T. Keyes, Mol. Phys., 37 (1979) 1413.

111. D. Samios, T. Dorfmuller, and A. Asembaum, Chem. Phys., 65 (1982) 305.

112. G. Huf-Desoyer, A. Asenbaum and M. Sedlacek, J. Chem. Phys., 70 (1979) 4924.

113. T. Dorfmuller, G. Fytas, W. Mersch and D. Samios, Faraday Symp. Chem. Soc., (1977) 11.

114. J. P. Munch and S. Candau, Mol. Motions Liq. Proc. Ann. Meet, Soc. Chim. Phys., 24th (1972) p. 535, ed. Lascombe.

115. K, Takagi, P. K. Choi, and K, Negishi J. Chem. Phys., 74 (1981) 1424.

116. K, Altenburg, Z. Phys. Chem., 250 (1972) 399.

117. R. Vallauri and M. Zoppi, Lett. Nuovo Cimento Soc. Ital. Fis., 9 (1974) 447.

118. A. Yoshihara, A. Anderson, R. A. Aziz and C. C. Lim, Chem. Phys., 61 (1981) 1.

119. M. Ferrario and M. W. Evans, Chem. Phys., in press, parts 1 and 2.

120. M. W. Evans, Adv. Mol, Rel. Int. Proc., in press.

121. Y. Y. Akhadov, "Dielectric Properties of Binary Solutions", Pergamon/Nauka, (1980), p. 397.

122. N. B. S. Circular No. 501.

123. C. A. Chatzidimitriou-Dreismann and E. Lippert, Ber. Buns. Phys. Chem., 84 (1980) 775.

124. C. A. Chatzidimitriou-Dreismann and E. Lippert, Croatica Chemica Acta, in press.

125. C. A. Chatzidimitriou-Dreismann, Thesis, Univ. of Berlin, 1982 (Iwan Stranski Institut).

126. R. Kubo, J. Phys. Soc. Japan, 12 (1957) 570.

127. K. M. van Vliet, J. Math. Phys., 19 (1978) 1345.

128. K. M. van Vliet, J. Math. Phys., 20 (1979) 2573.

129. N. G. van Kampen, Physica Narvegica, 5 (1971) 279; Fortschr. Physik, 4 (1956) 405; Physica, 29 (1954) 603; "Fundamental Problems in Statistical Mechanics of Irreversible Processes" in E.G.D. Cohen (ed.), "Fundamental Problems in Statistical Mechanics", N. G. van Kampen, Amsterdam, North-Holland, 1962, pp. 173-202.

130. M. Giordano, P. Grigolini and P. Marin, Chem. Phys. Lett., 83 (1981) 554.

131. P. Grigolini, Il Nuovo Cim., 63B (1981) 174.

132. S. Faetti, P. Grigolini, and F. Marchesoni, Z. Phys. B, in press.

133. P. Grigolini, Phys. Letters, 84A (1981) 301; Chem. Phys., 38 (1979) 389.

134. T. Fonseca, P. Grigolini and P. Marin, Phys. Lett., 88A (1982) 117.

135. M. Ferrario and P. Grigolini, J. Math. Phys., 20 (1979) 2567.

136. M. W. Evans, P. Grigolini and L. Resca, Chem. Phys. Lett., 47 (1977) 483.

137. P. Grigolini, Chem. Phys. Letters 47 (1977) 483.

138. P. Grigolini, and A. Lami, Chem. Phys., 30 (1978) 61.

139. U. Balucani, V. Tognetti, R. Vallauri, P. Grigolini and M. P. Lombardo, Phys. Letters, 86A (1981) 426.

140. M. Ferrario and P. Grigolini, J. Chem. Phys., 74 (1981) 235.

141. P. Grigolini, J. Stat. Phys., 27 (1982) 283.

142. I. Laulight and S. Meirman, J. Chem. Phys., 59 (1973) 2521.